

## Revealing the dual nature of magnetism in iron pnictides and iron chalcogenides using x-ray emission spectroscopy

H. Gretarsson,<sup>1</sup> A. Lupascu,<sup>1</sup> Jungho Kim,<sup>2</sup> D. Casa,<sup>2</sup> T. Gog,<sup>2</sup> W. Wu,<sup>1</sup> S. R. Julian,<sup>1</sup> Z. J. Xu,<sup>3</sup> J. S. Wen,<sup>3</sup> G. D. Gu,<sup>3</sup> R. H. Yuan,<sup>4</sup> Z. G. Chen,<sup>4</sup> N.-L. Wang,<sup>4</sup> S. Khim,<sup>5</sup> K. H. Kim,<sup>5</sup> M. Ishikado,<sup>6</sup> I. Jarrige,<sup>6</sup> S. Shamoto,<sup>6</sup> J.-H. Chu,<sup>7</sup> I. R. Fisher,<sup>7</sup> and Young-June Kim<sup>1,\*</sup>

<sup>1</sup>*Department of Physics, University of Toronto, 60 St. George St., Toronto, Ontario M5S 1A7, Canada*

<sup>2</sup>*Advanced Photon Source, Argonne National Laboratory, Argonne, Illinois 60439, USA*

<sup>3</sup>*CMP&MS Department, Brookhaven National Laboratory, Upton, New York 11973, USA*

<sup>4</sup>*Beijing National Laboratory for Condensed Matter Physics, Institute of Physics, Chinese Academy of Sciences, Beijing 100190, China*

<sup>5</sup>*CeNSCMR, Department of Physics and Astronomy, Seoul National University, Seoul 151-747, Republic of Korea*

<sup>6</sup>*Quantum Beam Science Directorate, Japan Atomic Energy Agency, Tokai, Naka, Ibaraki 319-1195, Japan*

<sup>7</sup>*Geballe Laboratory for Advanced Materials and Department of Applied Physics, Stanford University, Stanford, California 94305, USA*

(Received 30 August 2011; published 22 September 2011)

We report a Fe K $\beta$  x-ray emission spectroscopy study of local magnetic moments in various iron-based superconductors in their paramagnetic phases. Local magnetic moments are found in all samples studied: PrFeAsO, Ba(Fe,Co)<sub>2</sub>As<sub>2</sub>, LiFeAs, Fe<sub>1+x</sub>(Te,Se), and A<sub>2</sub>Fe<sub>4</sub>Se<sub>5</sub> (where A = K, Rb, and Cs). The moment size is independent of temperature or carrier concentration but varies significantly across different families. Specifically, all iron pnictide samples have local moments of about 1 $\mu_B$ /Fe, while FeTe and K<sub>2</sub>Fe<sub>4</sub>Se<sub>5</sub> families have much larger local moments of  $\sim 2\mu_B$ /Fe and  $\sim 3.3\mu_B$ /Fe, respectively. Our results illustrate the importance of multiorbital physics in describing magnetism of these compounds.

DOI: [10.1103/PhysRevB.84.100509](https://doi.org/10.1103/PhysRevB.84.100509)

PACS number(s): 74.70.Xa, 75.20.Hr, 78.70.En, 74.25.Ha

The duality of the local moment–itinerant electron in magnetism has long been confounding researchers trying to explain metallic ferromagnets such as Fe and Ni,<sup>1–3</sup> and it is again at the center of debate regarding microscopic understanding of magnetism in iron-based superconductors.<sup>4–9</sup> Various theoretical studies have approached magnetism in these materials from the itinerant viewpoint. In particular, density functional theory (DFT) predicted a spin-density-wave-type magnetic order in La(O<sub>1-x</sub>F<sub>x</sub>)FeAs,<sup>10–12</sup> which was later confirmed by neutron scattering experiments.<sup>13</sup> Despite this success, a fully itinerant description seems to be insufficient. For example, DFT calculations consistently overestimate the ordered magnetic moment of the parent compounds of iron pnictides. The theoretical value of  $\sim 2\mu_B$  (per Fe atom throughout this Rapid Communication)<sup>14</sup> is much larger than the ordered moment determined from neutron diffraction experiments.<sup>5</sup> Such a discrepancy has been attributed to the magnetic frustration and fluctuation effects from the local moment perspective.<sup>15,16</sup> Perhaps more pertinent to our discussion of the dual nature is the magnetic behavior in the paramagnetic regime. In the purely itinerant picture, the local magnetic moment would disappear above the transition temperature in zero field (Pauli paramagnet), while in the local picture (Curie paramagnet), local moments would be fluctuating and pointing in random directions. Therefore, the presence of local moments in the paramagnetic phase would be a telltale sign of localized magnetism.

However, experimentally probing local magnetic moments is challenging. The temperature dependence of spin susceptibility measured with magnetometry or NMR typically is strongly affected by the spin correlation, especially in iron pnictides and chalcogenides, in which the magnetic interaction energy scale is quite large.<sup>6</sup> Neutron scattering is useful and has been used to detect local moments,<sup>17–19</sup> but usually it is

time consuming and requires a large quantity of sample. Here we introduce x-ray emission spectroscopy (XES), which is a bulk-sensitive method to detect the local magnetic moment of Fe.<sup>20–24</sup> This XES technique is widely used in earth sciences to probe spin states of iron in minerals.<sup>22</sup> A recent development in quantitative analysis has made it possible to obtain local magnetic moment information without detailed line-shape analysis.<sup>21</sup>

In this Rapid Communication, we report our comprehensive XES investigation of magnetic moments in a number of iron pnictides and iron chalcogenides: PrFeAsO, Ba(Fe,Co)<sub>2</sub>As<sub>2</sub>, LiFeAs, Fe<sub>1+x</sub>(Te,Se), and A<sub>2</sub>Fe<sub>4</sub>Se<sub>5</sub> (where A = K, Rb, and Cs).<sup>25</sup> We find that local moments are present at room temperature in all samples studied. Furthermore, the size of the local moments vary significantly among the samples studied, ranging from 0.9 $\mu_B$  in LiFeAs to 3.3 $\mu_B$  in K<sub>2</sub>Fe<sub>4</sub>Se<sub>5</sub>. This result suggests that the magnetism in iron-based superconductors requires a description taking into account the local moment as well as the Fermi surface nesting. The relative importance of local moment versus itinerant magnetism depends on the type of anions and the structural details. Specifically, A<sub>2</sub>Fe<sub>4</sub>Se<sub>5</sub> is almost entirely described by local moments, while the local moment size decreases for Fe<sub>1+x</sub>(Te,Se) and is greatly suppressed for the pnictides samples. However, the variation of the magnetic moment size among the Fe pnictides (111, 122, and 1111) is found to be very small. We also discuss the possible origin of such a material dependence in view of the recent theoretical study by Yin *et al.*, in which magnetic moments were discussed in relation to orbital occupancy.<sup>9</sup>

XES was performed at the Advanced Photon Source on the undulator beamline 9ID-B. The beam was monochromatized by a double-bounce Si(111) crystal and a Si(311) channel-cut secondary crystal. A spherical (1 m radius) diced Ge(620)

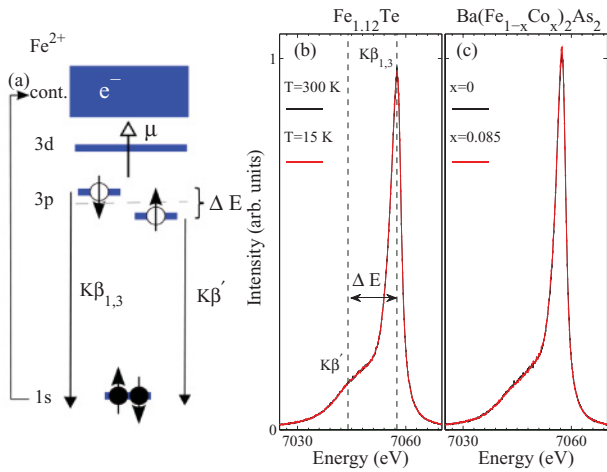


FIG. 1. (Color online) (a) Schematic diagram of the Fe  $K\beta$  emission process in the atomic limit for  $\text{Fe}^{2+}$ . The spin of the  $3p$  core-hole in the final state interacts with the net magnetic moment  $\vec{\mu}$  in the  $3d$  valence shell, creating two different final states  $K\beta_{1,3}$  and  $K\beta'$  with opposite core-hole spins, separated in energy by  $\Delta E$ . (b)  $K\beta$  emission line for  $\text{Fe}_{1.12}\text{Te}$  taken above and below  $T_N = 58$ . The splitting,  $\Delta E$ , between  $K\beta_{1,3}$  and  $K\beta'$  is caused by the local magnetic moment. (c)  $K\beta$  emission line for  $\text{BaFe}_2\text{As}_2$  for different Co doping.

analyzer was used to obtain an overall energy resolution of 0.4 eV (FWHM of the elastic line). The energy calibration was based on the absorption spectrum through a thin Fe foil, and incident x-ray energy of 7.140 keV was used. Use of such hard x-rays ensures that the spectra are not surface sensitive. Details of the growths and characterization of the single-crystal samples have been reported in earlier publications.<sup>26–30</sup> All measurements were carried out at room temperature, except for the temperature-dependence study, for which a closed-cycle cryostat was used.

The local moment sensitivity of the  $K\beta$  emission line ( $3p \rightarrow 1s$ ) originates from a large overlap between the  $3p$  and  $3d$  orbitals. In Fig. 1(a) we show a schematic diagram of the process for  $\text{Fe}^{2+}$  in the atomic limit. The  $K\beta$  emission process has a core-hole in the final state ( $3p^5$ ) which interacts strongly with the  $3d^6$  valence electrons, affecting the possible final-state configurations of the  $K\beta$  spectra.<sup>31,32</sup> In particular, such exchange interactions are mainly driven by the presence of a net magnetic moment in the  $3d$  valence shell, resulting in final states with antiparallel or parallel net spins between the  $3p^5$  core-hole and  $3d^6$  valence shell, as shown in Fig. 1(a). Since the  $3p$ - $3d$  interaction is local, this method is not sensitive to the long-range order but only probes the local magnetic moment. The two main multiplet features can be recognized in the  $K\beta$  emission line as the main peak  $K\beta_{1,3}$  and the low-energy satellite  $K\beta'$ , respectively. An example of such a splitting in the  $K\beta$  emission line for  $\text{Fe}_{1.12}\text{Te}$  is seen in Fig. 1(b), in which the splitting between the two features,  $\Delta E$ , was found to be  $\sim 13.25$  eV. The size of this splitting depends on the local moment,<sup>31</sup> but actually extracting the satellite peak position from fitting is quite difficult for a system with a weak moment [see Fig. 1(c)]. Bondino *et al.* used a similar splitting seen in the  $3s$ -core-level photoemission spectra to obtain a local moment of about  $1\mu_B$  in  $\text{CeFeAsO}_{0.89}\text{F}_{0.11}$ .<sup>33</sup>

Recently, a quantitative method based on the integration of the spectral weight difference has been suggested as a way to determine the local moment.<sup>21</sup> Since both the intensity of the satellite and the splitting  $\Delta E$  are related to the  $3d$  local moment,<sup>31</sup> this integrative method utilizes the whole spectrum and not just the peak position. The method has been successfully used in a number of applications.<sup>22–24</sup> In order to quantitatively derive the total local moment from the  $K\beta$  line using the integrated absolute difference (IAD) analysis, one needs to have a reference sample with the same local coordination around Fe, but with Fe ion in the nonmagnetic low-spin (LS) state. The IAD is then the integrated absolute difference between the spectrum measured and the nonmagnetic reference spectra. Vanko *et al.*<sup>21</sup> showed that the IAD is linearly proportional to the spin magnetic moment of the Fe atom. For this purpose, we use  $\text{FeCrAs}$  as a nonmagnetic reference sample. The Fe atoms in  $\text{FeCrAs}$  are tetrahedrally coordinated with As, as is found in Fe superconductors. Although  $\text{FeCrAs}$  orders magnetically, both experimental<sup>34</sup> and theoretical<sup>35</sup> studies have shown that the magnetism entirely resides on the Cr sites, and Fe is nonmagnetic. In order to determine the absolute scale of the magnetic moment, we use the value for the Fe-chalcogenide  $\text{K}_2\text{Fe}_4\text{Se}_5$ . Since this is an insulating sample, we assume that the local moment size is the same as the ordered magnetic moment at room temperature; both neutron scattering<sup>36</sup> and DFT calculation<sup>37</sup> results agree on the value of the ordered magnetic moment of  $3.3\mu_B$ .

In Fig. 2 we show representative  $K\beta$  XES data for (a)  $\text{LiFeAs}$ , (b)  $\text{PrFeAsO}$ , (c)  $\text{Fe}_{1.05}\text{Te}$ , and (d)  $\text{K}_2\text{Fe}_4\text{Se}_5$  along with the  $\text{FeCrAs}$  spectrum. To follow the procedure from Ref. 21, the area underneath each spectrum was normalized

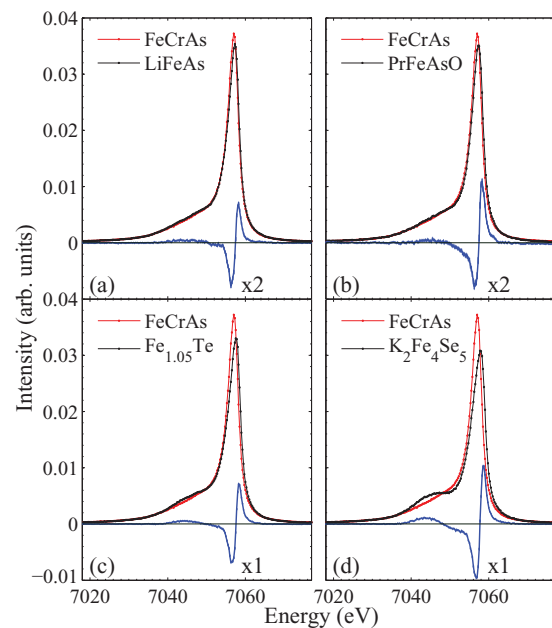


FIG. 2. (Color online) The XES spectra of the Fe  $K\beta$  emission lines for (a)  $\text{LiFeAs}$ , (b)  $\text{PrFeAsO}$ , (c)  $\text{Fe}_{1.05}\text{Te}$ , and (d)  $\text{K}_2\text{Fe}_4\text{Se}_5$ . The nonmagnetic reference spectra of  $\text{FeCrAs}$  and the difference spectra are also plotted. Note that the difference spectrum for both  $\text{LiFeAs}$  and  $\text{PrFeAsO}$  were magnified by a factor of 2.

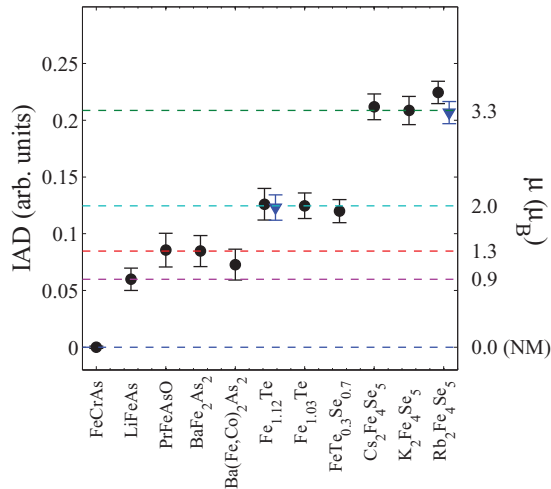


FIG. 3. (Color online) The IAD values derived from the XES spectra for various samples. The room-temperature data are shown in circles, and the low-temperature IAD values at  $T = 15$  K are shown in triangles for  $\text{Fe}_{1.12}\text{Te}$  and  $\text{Rb}_2\text{Fe}_4\text{Se}_5$ . On the right-hand side is the local magnetic moment ( $\mu$ ) scale.

to unity. The reference spectrum is then subtracted from the sample spectrum, and the resulting difference is plotted. The IAD quantity is extracted by integrating the absolute value of this difference spectrum. What is evident from Fig. 2 is that the intensity of  $K\beta'$  changes quite a bit going from  $\text{PrFeAsO}$  to  $\text{K}_2\text{Fe}_4\text{Se}_5$ . In addition we see a shift of the main  $K\beta_{1,3}$  peak position toward higher energy as  $K\beta'$  increases in intensity, providing further evidence of the local moment variation.<sup>21</sup>

The IAD values so obtained for all the samples are plotted in Fig. 3. On the right-hand side of the figure is the local moment scale determined from the  $\text{K}_2\text{Fe}_4\text{Se}_5$  ordered moment.<sup>36</sup> The moment sizes roughly falls within three groups. All  $\text{AFe}_2\text{Se}_2$  samples have approximately the same moment size close to  $3.3\mu_B$ , while the local moment size for all  $\text{Fe}(\text{Te},\text{Se})$  samples is around  $2\mu_B$ . Both of these values are close to the respective ordered moment size but are much larger than the values for Fe pnictides, which carry local moments of about  $1\mu_B$ . This latter value is quite similar to the ordered moment reported for  $\text{BaFe}_2\text{As}_2$  ( $0.9\mu_B$ )<sup>38</sup> but much larger than the values for  $\text{PrFeAsO}$  and  $\text{LiFeAs}$ . The ordered moment size for  $\text{PrFeAsO}$  is  $0.35\mu_B$  (Ref. 39) and  $\text{LiFeAs}$  does not order magnetically; isostructural  $\text{NaFeAs}$  has an ordered moment of  $0.09\mu_B$ .<sup>40</sup> Our results of the local moments in Fe pnictides are also larger than that reported in Mössbauer spectroscopy studies (e.g., an ordered moment of  $\sim 0.3\mu_B$  was found for  $\text{PrFeAsO}$ <sup>41</sup>). Since the moment size determined from the XES is the local moment in the paramagnetic phase, it differs from the long-range ordered moment seen with neutron scattering or Mössbauer spectroscopy.

We also studied the temperature and carrier doping dependence of the local moment size or lack thereof. In Fig. 1(b), we show XES spectra for  $\text{Fe}_{1.12}\text{Te}$  obtained at two different temperatures above and below the magnetic ordering transition ( $T_N \approx 58$  K). In Fig. 1(c), the  $\text{Ba}(\text{Fe}_{0.915}\text{Co}_{0.085})_2\text{As}_2$  XES spectrum is compared with that of undoped  $\text{BaFe}_2\text{As}_2$  compound. The magnetic order is

suppressed in the  $\text{Ba}(\text{Fe}_{0.915}\text{Co}_{0.085})_2\text{As}_2$  sample, which is superconducting with  $T_c \approx 17$  K. The lack of any change in both figures indicates that the local moment size is insensitive to the presence of long-range order or carrier concentration. A similar conclusion can be reached from additional temperature and doping dependence studies for  $\text{Rb}_2\text{Fe}_4\text{Se}_5$  and  $\text{FeTe}_{0.3}\text{Se}_{0.7}$  (included in Fig. 3). This is in contrast to recent neutron scattering results, in which increased moment size in the paramagnetic phase of  $\text{Fe}_{1.1}\text{Te}$  was observed.<sup>18</sup> In the case of  $\text{Rb}_2\text{Fe}_4\text{Se}_5$  the lack of change above and below the superconducting  $T_c = 30$  K is in agreement with neutron scattering experiments,<sup>36</sup> in which a large local moment ( $\sim 3.3\mu_B$ ) was found to exist in the superconducting phase, although this could be due to a phase separation as suggested in recent studies.<sup>42–44</sup>

Summarizing our experimental findings, we have found local magnetic moments in the paramagnetic phase of all Fe pnictides and chalcogenides samples. In addition, the local moment size only depends on which anion the sample has and is insensitive to doping and temperature. In particular, we find that the local moment size varies very little among the three ferropnictides families, despite widely different ordered moment size. In their recent dynamical mean field theory (DMFT) calculation combined with DFT, Yin *et al.* found that the paramagnetic fluctuating local moment was rather sample independent among the 111, 1111, and 122 families of iron pnictides,<sup>9</sup> which is consistent with our experimental observation. However, the fluctuating local moment from the calculation ( $\sim 2.4\mu_B$ ) is still larger than the observed  $1\mu_B$  for ferropnictides, implying that there exist “missing” magnetic moments. We speculate that XES is weighted such that local electrons are emphasized while more itinerant electrons are not properly counted, due to the local nature of the core-hole potential. It has been theoretically suggested that different orbitals might have different degrees of localization.<sup>8,9</sup>

On the other hand, the calculated fluctuating moment size of the 11 iron chalcogenides agrees fairly well with our XES value ( $\sim 2\mu_B$ ). In addition, the local moment size was found to be similar in both  $\text{FeTe}$  and  $\text{FeSe}$ , even though the long-range order is lost in  $\text{FeSe}$ . These results are in agreement with our results in Fig. 3 in which no difference was seen in the IAD values for  $\text{Fe}_{1.12}\text{Te}$ ,  $\text{Fe}_{1.05}\text{Te}$ , and  $\text{FeTe}_{0.3}\text{Se}_{0.7}$ . Yin and co-workers suggested that the structural details of the Fe-pnictogen/chalcogen tetrahedra are crucial in determining the orbital occupancy and the quasiparticle mass enhancement, which in turn determines the magnetic moment.<sup>9</sup> In particular, the large Te ions make this system structurally distinct from ferropnictides.

In conclusion, we find that  $\text{PrFeAsO}$ ,  $\text{Ba}(\text{Fe},\text{Co})_2\text{As}_2$ ,  $\text{LiFeAs}$ ,  $\text{Fe}_{1+x}(\text{Te},\text{Se})$ , and  $\text{A}_2\text{Fe}_4\text{Se}_5$  (where  $A = \text{Cs}, \text{K},$  and  $\text{Rb}$ ) all possess local magnetic moments even in their paramagnetic phases. By analyzing our x-ray emission spectroscopy data using a recently developed integrated absolute difference method, we could determine the local moment size for each sample. The local moment sizes of iron chalcogenides agree with the theoretical calculation values and experimentally measured static moment sizes. However, the local moment size of ferropnictides is universally around  $1\mu_B$ , which could originate from the more localized  $t_{2g}$  electrons. Our results

perhaps suggest that it is the  $t_{2g}$  local moment that orders in ferropnictides, eliminating the need for Fermi-surface nesting, as argued in a recent theoretical study.<sup>4</sup>

We would like to thank H. Eisaki and A. Iyo for fruitful discussion and technical assistance with the PFAO crystal growth. Research at the University of Toronto was supported by the NSERC, CFI, OMRI, and ClfAR. Y.-J.K. was supported by the KOFST through the Brainpool program. Use of the APS was supported by the U.S. Department of Energy, Office of Science,

Office of Basic Energy Sciences (BES), under Contract No. W-31-109-ENG-38. The work at Brookhaven National Laboratory was supported by the U.S. Department of Energy under Contract No. DE-AC02-98CH10886. N.-L.W. acknowledges NSFC and the MOST 973 project from China. Work at Seoul National University, was supported by the National Creative Research Initiative (2010-0018300). Work at the Japan Atomic Energy Agency was supported by JST, TRIP. Work at Stanford was supported by the U.S. Department of Energy, Office of BES, under Contract No. DE-AC02-76SF00515.

\*yjkim@physics.utoronto.ca

<sup>1</sup>A. Kakizaki, J. Fujii, K. Shimada, A. Kamata, K. Ono, K. H. Park, T. Kinoshita, T. Ishii, and H. Fukutani, *Phys. Rev. Lett.* **72**, 2781 (1994).

<sup>2</sup>M. Pickel, A. B. Schmidt, M. Weinelt, and M. Donath, *Phys. Rev. Lett.* **104**, 237204 (2010).

<sup>3</sup>A. I. Lichtenstein, M. I. Katsnelson, and G. Kotliar, *Phys. Rev. Lett.* **87**, 067205 (2001).

<sup>4</sup>M. D. Johannes and I. I. Mazin, *Phys. Rev. B* **79**, 220510(R) (2009).

<sup>5</sup>M. D. Lumsden and A. D. Christianson, *J. Phys. Condens. Matter* **22**, 203203 (2010).

<sup>6</sup>D. C. Johnston, *Adv. Phys.* **59**, 803 (2010).

<sup>7</sup>J. Hu, e-print [arXiv:1106.5169v1](https://arxiv.org/abs/1106.5169v1).

<sup>8</sup>J. Wu, P. Phillips, and A. H. Castro Neto, *Phys. Rev. Lett.* **101**, 126401 (2008).

<sup>9</sup>Z. P. Yin, K. Haule, and G. Kotliar, e-print [arXiv:1104.3454v1](https://arxiv.org/abs/1104.3454v1).

<sup>10</sup>D. J. Singh and M. H. Du, *Phys. Rev. Lett.* **100**, 237003 (2008).

<sup>11</sup>J. Dong *et al.*, *Europhys. Lett.* **83**, 27006 (2008).

<sup>12</sup>I. I. Mazin, D. J. Singh, M. D. Johannes, and M. H. Du, *Phys. Rev. Lett.* **101**, 057003 (2008).

<sup>13</sup>C. de la Cruz *et al.*, *Nature (London)* **453**, 899 (2008).

<sup>14</sup>See, e.g., C. Cao, P. J. Hirschfeld, and H. P. Cheng, *Phys. Rev. B* **77**, 220506 (2008).

<sup>15</sup>T. Yildirim, *Phys. Rev. Lett.* **101**, 057010 (2008).

<sup>16</sup>Q. Si and E. Abrahams, *Phys. Rev. Lett.* **101**, 076401 (2008).

<sup>17</sup>S. O. Diallo *et al.*, *Phys. Rev. B* **81**, 214407 (2010).

<sup>18</sup>I. A. Zaliznyak *et al.*, e-print [arXiv:1103.5073v1](https://arxiv.org/abs/1103.5073v1).

<sup>19</sup>Z. Xu *et al.*, e-print [arXiv:1012.2300v1](https://arxiv.org/abs/1012.2300v1).

<sup>20</sup>J.-P. Rueff, C. C. Kao, V. V. Struzhkin, J. Badro, J. Shu, R. J. Hemley, and H. K. Mao, *Phys. Rev. Lett.* **82**, 3284 (1999).

<sup>21</sup>G. Vanko *et al.*, *J. Phys. Chem. B* **110**, 11647 (2006).

<sup>22</sup>J. F. Lin *et al.*, *Science* **317**, 1740 (2007); J. F. Lin *et al.*, *Nature Geosci.* **10**, 1038 (2008).

<sup>23</sup>U. Bergmann and P. Glatzel, *Photosynth. Res.* **102**, 255 (2009).

<sup>24</sup>J.-P. Rueff, M. Mezouar, and M. Acet, *Phys. Rev. B* **78**, 100405(R) (2008).

<sup>25</sup>Actual compositions for these compounds are  $K_{0.83}Fe_{1.53}Se_2$ ,  $Rb_{0.8}Fe_{1.7}Se_2$ , and  $Cs_2Fe_4Se_5$ .

<sup>26</sup>J.-H. Chu, J. G. Analytis, C. Kucharczyk, and I. R. Fisher, *Phys. Rev. B* **79**, 014506 (2009).

<sup>27</sup>M. Ishikado *et al.*, *Physica C* **469**, 901 (2009).

<sup>28</sup>Z. G. Chen *et al.*, *Phys. Rev. B* **83**, 220507(R) (2011).

<sup>29</sup>W. Wu *et al.*, *Solid State Phenom.* **170**, 276 (2011).

<sup>30</sup>B. Lee *et al.*, *Europhys. Lett.* **91**, 67002 (2010).

<sup>31</sup>K. Tsutsumi *et al.*, *Phys. Rev. B* **13**, 929 (1976).

<sup>32</sup>G. Peng *et al.*, *J. Am. Chem. Soc.* **116**, 2914 (1994).

<sup>33</sup>F. Bondino *et al.*, *Phys. Rev. Lett.* **101**, 267001 (2008).

<sup>34</sup>W. Wu *et al.*, *Europhys. Lett.* **85**, 17009 (2009).

<sup>35</sup>S. Ishida *et al.*, *Physica B* **217**, 87 (1996).

<sup>36</sup>W. Bao *et al.*, *Chin. Phys. Lett.* **28**, 086104 (2011); e-print [arXiv:1102.3674v1](https://arxiv.org/abs/1102.3674v1).

<sup>37</sup>X. W. Yan *et al.*, *Phys. Rev. B* **83**, 233205 (2011).

<sup>38</sup>S. D. Wilson, Z. Yamani, C. R. Rotundu, B. Freelon, E. Bourret-Courchesne, and R. J. Birgeneau, *Phys. Rev. B* **79**, 184519 (2009).

<sup>39</sup>S. A. J. Kimber *et al.*, *Phys. Rev. B* **78**, 140503 (2008).

<sup>40</sup>S. L. Li, C. de la Cruz, Q. Huang, G. F. Chen, T. L. Xia, J. L. Luo, N. L. Wang, and P. Dai, *Phys. Rev. B* **80**, 020504 (2009).

<sup>41</sup>M. A. McGuire *et al.*, *New J. Phys.* **11**, 025011 (2009).

<sup>42</sup>F. Chen *et al.*, e-print [arXiv:1106.3026v1](https://arxiv.org/abs/1106.3026v1).

<sup>43</sup>W. Li *et al.*, e-print [arXiv:1108.0069v1](https://arxiv.org/abs/1108.0069v1).

<sup>44</sup>R. H. Yuan *et al.*, e-print [arXiv:1102.1381v3](https://arxiv.org/abs/1102.1381v3).